

## Phase equilibria, phase changes, and mesophases: Analysis and simulation

---

The conclusion we have reached is a special case of one of the most elegant results of chemical thermodynamics. The phase rule was derived by Gibbs and states that, for a system at equilibrium,  $F=C - P + 2$ .

Atkins, P. W. *The Elements of Physical Chemistry*, 2001, 3rd ed, Oxford University Press, p.195; as elegant as useless.

### 13.1 Things and molecules

The story, or the myth, goes that when somebody asked Enrico Fermi if he knew the thermal conductivity of some metal, or if he could remember the mathematical equation for a given phenomenon, he would say “no”, and then proceed to derive the requested information from first principles. Now there is no question that Fermi mastered the principles of physics in the same way as that Maurizio Pollini masters the keyboard of his piano, but there is also no question that there must be a certain amount of exaggeration in the story.

A normal person wakes up in the morning, yawns, gets out of bed, has a cup of coffee, chews a doughnut, lathers his chin to shave, dresses, climbs into his car, and drives to work. A chemist has his brain triggered to attention by the release of several neurotransmitter molecules, including serotonin and acetylcholine, sends an electric signal to his muscle activators to compress the lung tissue in order to pull in a 20% oxygen–nitrogen gas mixture and to stretch his legs, stimulates his taste receptors with a water solution made of caffeine, sucrose and an enormous amount of trace aromatic molecules, uses the saliva enzymes to degrade a piece of polysaccharide, fills the pores of his chin with a gas/liquid suspension of surfactant molecules, then protects his skin with a 60–40% coating of silk and polymer fibers, impregnated with appropriate dyes to make them attractive, and finally ignites a gasoline/air mixture to generate heat which forces a gas to expand, pumping some pistons up and down and chug-chugging his car along. What a complicated life. But like Enrico Fermi, chemists refuse to take objects at their face value and prefer to work their way from atoms and molecules to the shape and properties of objects as we see them. The structure–activity principle does the rest, and this attitude makes the chemist the master of the world. This is admittedly a very cavalier attitude and no doubt frustration is much more

common than success, but the molecular point of view is certainly the cast of mind of the chemistry of the years and centuries to come.

All matter, from the simplest fluid such as gaseous helium to the most complex system like a biological cell, is made of electrons and nuclei. Electric potentials tend to glue the nuclei together, while kinetic energy, connected to atomic (nuclear) masses moving with given velocities, tends to pull them apart. It is this eternal struggle between electricity and temperature that ultimately gives rise to the entire world as we see it, with its properties and its changes. This chapter examines a portion of this extremely wide and complicated landscape, within the following limitations.

1. Chemical bonding is not considered, i.e. molecules are taken as they are and do not react.
2. The analysis is limited to compounds made of the usual elements of organic chemistry, with the exclusion of organometallics, rocks, silicates, and metals.
3. Molecules are considered only up to a size of some 1000 da, with the exclusion of polymers and biological macromolecules.
4. Only pure substances or binary mixtures are considered.

Within the above-mentioned restrictions, a phase is a piece of matter containing one or two chemical species in a distinguishable state of aggregation. Admittedly, this oversimplifies the real world, where even one of the purest liquids, drinking water, is a solution of hundreds of components, and most chemical systems consist of many different chemicals in different and perhaps variable states of aggregation.

## 13.2 Basic thermodynamic functions

The basic thermodynamic functions enthalpy, heat capacity, and entropy are strongly dependent on the state of aggregation. Enthalpy and heat capacity are higher in condensed states because of the significant intermolecular potential energy terms, and increase with the number of vibrational energy “pockets” available (recall equations 7.25 and 7.30); for example in a periodic solid the partition function includes sums over vibrational states in the whole Brillouin zone (see Section 6.3). Entropy is proportional to the amount of phase space which the system can explore, and the higher dispersion in space for gases largely overweighs the dispersion of energy among available states, which are more numerous in condensed systems. Hence the familiar rule:

$$H_{\text{cr}} > H_{\text{l}} > H_{\text{g}}; \quad S_{\text{g}} > S_{\text{l}} > S_{\text{cr}}; \quad C_{\text{p,l}} > \sim C_{\text{p,cr}} > C_{\text{p,g}}$$

The thermodynamic treatment of equilibrium is in terms of chemical potentials. Phase equilibria and phase changes are dictated by the leverage between enthalpic and entropic terms implicit in equations such as 7.49 and 7.55. Such equations, however, hold exactly for infinite and homogenous systems, but in real systems the influence of size, termination, and defects cannot be neglected. The microscopic texture of the system may then become of paramount importance, and it must be said at once that this is

the case for most of the chemical phenomena and transformations in phase transitions. Size and heterogeneity can be incorporated in the thermodynamic treatment through surface free energies, but if the measurement of thermodynamic functions is not easy for homogeneous and continuous systems, it is orders of magnitude more awkward for surface-dependent systems. The very concept of chemical equilibrium may dissolve across a maze of semi- or non-equilibrium states, and the derived equations show an unpleasant dependence from poorly characterized boundary conditions, or from the chemical constitution of each system, if not altogether from the particular working conditions of each experiment, with a loss of generality that does much harm to the development of fundamental knowledge. One often hears of a crucial role played by “activation free energies”, quantities whose very name casts a shadow of uncertainty by its admixture of thermodynamic and kinetic flavors. There is very little that can be done against this state of affairs.

### 13.3 Melting

Consider as a first example a piece of pure crystalline solid in equilibrium with its pure liquid, at the melting temperature. Assume that the crystals are large enough that surface effects can be neglected (as will become clear later, this is quite an assumption). If an amount of heat that is less than the latent heat corresponding to the crystal mass is supplied to the system, some crystalline material will melt at equilibrium without change in temperature, but as soon as more heat is poured into the system, after all the solid mass has melted the heat can be used to raise the temperature, the chemical potential of the crystal exceeds that of the liquid, and the crystal becomes thermodynamically unstable. The reasoning seems neat and simple, but if one tries to work it backwards, and expect crystallization after subtracting the appropriate amount of heat, kinetics sets in and supercooling is the rule rather than the exception, with the sample staying liquid for a long time well below the melting temperature, especially if the cooling rate is very slow. The reason is of course that it takes a comparatively long time for molecules to find their way through phase space and lock into the proper reciprocal orientation for crystallization. Equilibrium thermodynamics compares different states in an abstract sense, and not the different states of the parts of a system that are actually undergoing a given chemical process.

The thermodynamic law that governs the solid–liquid equilibrium is equation 7.57, so that the equilibrium melting temperature is a ratio of melting enthalpy to melting entropy.  $T_m$  and  $\Delta H_m$  can be measured fairly easily (Section 7.6), so that equilibrium melting entropies can also be obtained. Is there a relationship between the melting temperature and the molecular structure or crystal forces? Intuitively, one would expect easier melting for less cohesive crystals, and, indeed, there seems to be some correlation between melting temperatures and sublimation enthalpy – surprisingly, a steadier correlation than with melting enthalpies [1]. A further view on this problem is provided by a statistical analysis of melting entropies. They are about  $13 \text{ J K}^{-1} \text{ mol}^{-1}$  for small spherical molecules (the translational contribution) and about  $57 \text{ J K}^{-1} \text{ mol}^{-1}$

for rigid molecules (Walden's rule). But there are fluctuations; according to one hypothesis [2], the more symmetrical a molecule, the higher its probability of being in the correct orientation to be incorporated into the crystal lattice, with a decrease in the difference between periodic crystal and randomly oriented liquid molecules, and a lowering of the melting entropy.  $\Delta S_m$  then consists of the translational contribution plus a rotational contribution of  $57 - 13 = 44 \text{ kJ mol}^{-1}$ , further corrected by a term in the logarithm of the rotational symmetry number,  $\sigma$  [2]:

$$\Delta S_m = 13 + [44 - R \ln(\sigma)] \quad (13.1)$$

With the assumption that melting enthalpies are much less affected by molecular symmetries, symmetric molecules must have higher melting points and lower ideal solubilities [3]. Although to some extent revealing, such correlations are mostly qualitative and hardly comprehensive [3,4] Entropy from conformational flexibility, blocked in the crystal and free in the liquid, is not considered.

Molecular shape also influences crystal properties and the thermodynamic melting parameters, sometimes in a simple and understandable way. Globular molecules tend to form plastic crystals, in which extensive reorientation of parts of the molecule or even of the entire molecule occurs, without substantial translational diffusion; the crystal is made of a periodic array of rotators. Clearly, the rotational contribution to the melting entropy is lower, as the crystal already possesses some of the rotational freedom of the liquid, so that  $\Delta S_m$  is depressed and the melting point is abnormally high. An example is provided by *tert*-butyl derivatives [5], whose crystals show a phase transition from a low-temperature, ordered phase II to a high-temperature, rotationally activated phase I, which then evolves into the liquid. Melting entropies are particularly low,  $5\text{--}15 \text{ J K}^{-1} \text{ mol}^{-1}$ , while the sum of the melting entropy and of  $\Delta S$  for the II-I transition is around  $40 \text{ J K}^{-1} \text{ mol}^{-1}$ , not far from the boundaries of equation 13.1. Rotational activation in the solid is also the common explanation of the unusually high melting temperature of planar, disk-like aromatic molecules, benzene being a classical example. All things considered, however, the melting temperature of an organic compound is one of the least predictable thermodynamic properties.

Some aspects of the melting process can be studied by evolutionary simulation methods like molecular dynamics [6]. A crystalline computational box is set up, and the system is gently driven up in computational temperature until evolution into the liquid state occurs. As an example of the output of such a computational experiment [7], Fig. 13.1 shows the evolution of the most important quantities (intermolecular potential energies and density) throughout the whole process for the benzene molecule. After sequential runs with increasing temperature, decreasing density, and decreasing cohesive energy, when the computational box is brought to 300 K, which is some 20 K above the experimental melting temperature, the melting catastrophe is almost instantaneous, and is revealed (recall Section 9.2) by a sudden drop in density and rise in potential energy. Note that the kinetic energy does not change because the temperature is promptly kept constant by a supply of computational heat from the T-coupling mechanism. The enthalpy of melting can be calculated from the difference in total energy between the equilibrated crystal and the equilibrated liquid.

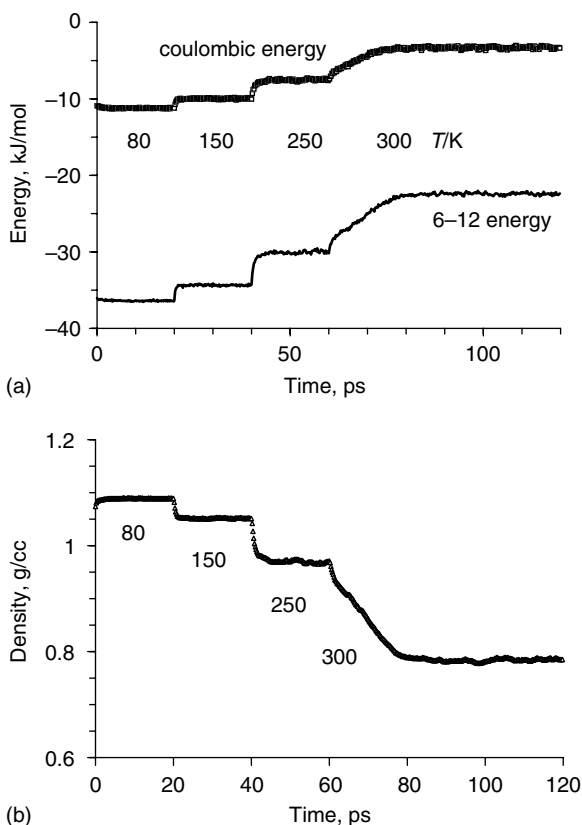


**Fig. 13.1.** (a) Time evolution of the 6–12 and coulombic potential energies during the simulation that goes from crystalline benzene at 80 K to liquid benzene at 300 K. The inset shows the temperatures of the simulations. The 60–80 ps section corresponds to the melting run. (b) Density profile along the same trajectories as in (a).

In the 60–80 ps section of Fig. 13.1 the benzene molecules are literally pushing the crystal lattice apart under the effect of the suddenly available kinetic energy. Diffusional and rotational freedom results and the crystal collapses to the liquid, which is then normally simulated at 300 K in the 80–120 ps section of the run. Since the part of the simulation where melting occurs is a non-equilibrium simulation, one cannot draw any conclusions from averages, nor can one claim to have simulated the actual solid–liquid equilibrium or to have predicted the melting temperature. Nevertheless, such dynamic runs offer a window over the evolution of the internal structure of the system as it goes from crystal to liquid; an example taken from a study of acetic acid is shown in Fig. 13.2. One cannot say for sure that this picture is a representation of the true structural changes that occur when the acetic acid crystal melts; molecular

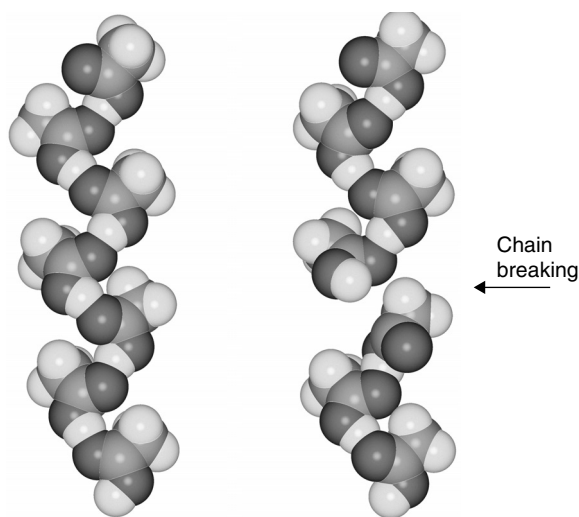


**Fig. 13.2.** Snapshots drawn from pre-melting trajectories for the acetic acid crystal. A regular chain of hydrogen-bonded molecules is seen on the left. On the right, one molecule has flipped around, breaking the chain and cross-linking to form a hydrogen bond to a neighboring chain (the arrow indicates the oxygen atom that is no longer engaged in intra-chain hydrogen bonding). After ref. [6a].

dynamics is only a simulation, and its results depend on the details of the potentials and of the computational setup; and yet, it offers a gallery of possible events, that become more and more realistic with increasing accuracy of the potentials and length of the simulation, and can be further examined by other experimental techniques. The role of molecular dynamics is often similar to that of a police officer who shows a gallery of photographs of possible culprits to the witness of a crime scene.

It has been shown [8] that in MD melting runs there is a no-return point, such that computational frames before that point revert to the crystal upon cooling, while frames after that point cannot be prevented from collapsing into the liquid. What this means in terms of structure is far from clear, and it is not even obvious that this crossover point is reproducible, as the effect must be to some extent dependent on the particular track through phase space taken by the simulation. In any case, computational experiments with the introduction of a small number of vacancies in the crystal lattice [6a] or on the melting of computational polymorphs with variable density [8] show that any decrease in the compactness and close packing of the crystalline material, even a very minor one, has huge consequences on the propensity towards melting, as expected.

There are many more ways in which molecular dynamics can be used to study the molecular events as a crystal structure approaches the melting point. Figure 13.3(a) shows the radial distribution function (see in Section 9.4.1) for the molecular centers of mass in the benzene crystal. As temperature rises, the peaks shift to longer separations

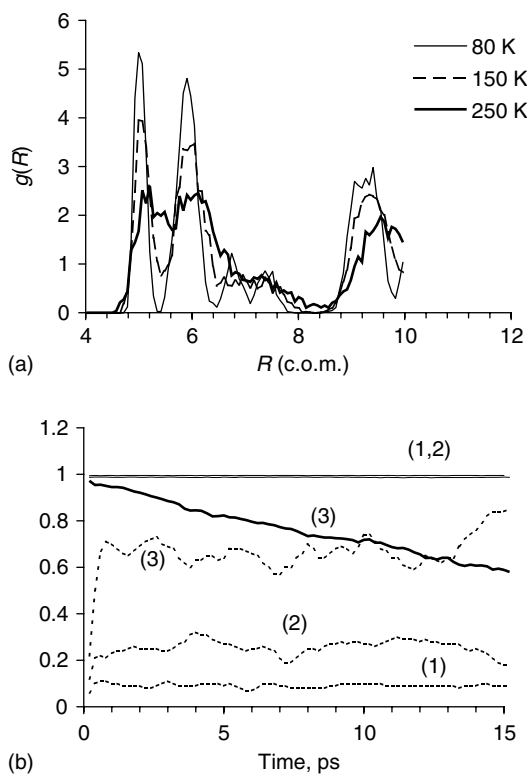


**Fig. 13.3.** (a) Radial distribution functions for the molecular centers of mass in the benzene crystal, from an MD simulation. (b) Same simulation: dashed lines, mean center of mass displacements; full lines: rotational correlation function for in-plane oscillation. (1), (2) and (3) at 80, 150 and 250 K respectively. The rotational function at 250 K shows the onset of molecular rotation.

and become flatter and wider, as a consequence of the increased displacement freedom due to the decrease in density (not unexpectedly; to pursue the previous criminal analogy further, presenting a picture of Al Capone to mafia prosecutors). Rotational correlation functions provide further information: Fig. 13.3(b) shows that at 250 K, even while the crystal remains integer, as testified by constant density and steady mean square displacements of the center of mass, there is a loss of orientational correlation for in-plane rotation, as the benzene crystal moves to a rotator phase by a second-order phase transition. This in-plane rotation of the molecules in the benzene crystal, so clearly pointed out by molecular dynamics, is confirmed by NMR relaxation experiments (recall Table 1.6 and the related discussion). Note that the loss of orientational correlation in the crystal is partial, and is on a much longer timescale (15 ps for a 0.4 decrease) than in the liquid state (Fig. 13.4, full loss in

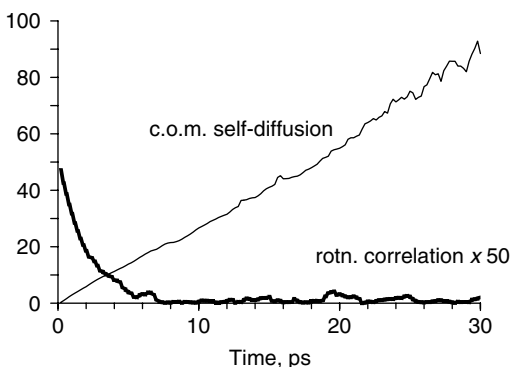


**Fig. 13.4.** Center of mass displacement and rotational correlation function for liquid benzene at 300 K. 80–120 ps section of the simulation shown in Fig. 13.1.

6 ps), demonstrating the directional constraint and the comparatively high activation barrier for the rotation in the crystal.

No wonder, the atomic details of the mechanism of melting are far from clear. Intuitively, one may recall that as temperature rises, the anharmonicity of the interatomic potential requires a decrease in density, so that at some point the molecules in the solid find enough space around them to become free to diffuse or rotate, with a consequent collapse of long range structural periodicity and a catastrophic evolution into the liquid state. The number (concentration) of these defects is a reproducible quantity at a given temperature. This so-called Lindemann criterion [9] sets a limiting value for the volume increase that the solid can withstand; this rule apparently holds for crystals made of simple spherical particles, which melt as soon as the vibrational amplitude exceeds 15% of the cubic cell edge. This is also the order of magnitude for the average volume increase on going from a very low temperature to the melting temperature for organic crystals (recall Fig. 11.4), but the formulation of a theory for this behavior would require at the very least an anisotropic version of the Lindemann rule, somehow taking into account also the wide variety of molecular shapes and interaction potentials – a very difficult path to follow.

A different mechanism, verified by careful experiments, is surface melting [10]: below the melting point, solid particles become coated with a liquid-like film of increasing thickness, in thermodynamic equilibrium with the solid, and it is this liquid-like portion of the system that functions as a trigger for the subsequent bulk melting. At the normal melting temperature, the melt front rushes in further, transforming the entire solid into a liquid. If this mechanism were always true and necessary, melting would be a surface-dependent phenomenon and an infinite bulk solid would never melt. In fact this mechanism certainly applies to systems made of very simple particles, like Ar atoms, but it is doubtful that it may be at work in complex molecular systems. Surface melting is a sort of extreme surface reconstruction, a phenomenon which may not be pervasive or even frequent for molecules with large and articulated

anchoring points. A logical conjecture is to propose that melting may initiate at any kind of defect (grain boundaries, dislocations, etc.), the surface being the most obvious “defect” in any real solid, but without the need for a real surface liquid layer. Anyway, the Lindemann criterion and surface melting are not mutually exclusive, and neither precludes the sharpness and reproducibility of the melting points of organic compounds, as they both result from equilibrium conditions that are met at well specified temperatures.

Molecules in crystals undergo collective oscillations (Section 6.3) whose frequency and associated librational energy are sharp functions of the boundary conditions imposed by the surrounding lattice. As density decreases with rising temperature, some of these conditions may in some cases become much less imposing or may eventually vanish, and the corresponding vibrations become “soft modes”. These soft modes lead to collective structural rearrangements and to crystal–crystal phase transitions with almost zero cost in enthalpy [11]. Is melting the result of some mode softening or even of a simultaneous softening of all lattice modes, or, as an alternative, of a chaotic loss of correlation at single defect points? No one can tell for sure, but the most disquieting side of this question is that there may not be a unique answer, except, once again, for crystals made of very simple objects such as hard spheres, disks, or cylinders. For example, the instabilities in *n*-alkane crystals above a certain temperature have been studied by molecular dynamics [12], leading to the conclusion that “the instabilities ... correspond to the softening of long-wavelength vibrational modes associated with rigid motion of the chains ... the instability then propagates to smaller wavelengths”. Conceivably, many different things may happen in the almost infinite variety of shapes and potentials represented in large and flexible organic molecules, and it may be extremely difficult if not altogether impossible to find general rules. The solid-state chemist is here in the position of the physicist who (so the story goes) when asked if she could provide a general equation for the motion of a horse, answered, yes, but only assuming a spherical horse.

### 13.4 Solid–liquid equilibrium and nucleation from the melt

If melting is difficult to characterize in molecular terms, nucleation and growth of crystalline particles from the melt is an even more elusive phenomenon. Given the extreme difficulty of obtaining molecular level information, phenomenological, macroscopic nucleation theories have been formulated [13] before and aside from numerical molecular simulation. These theories constitute an almost completely parallel approach to the matter and their description does not belong in this book, although points of contact with molecular level simulations have been explored [14].

The following treatment of nucleation in classical nucleation theory (CNT) provides a glimpse of the methods and reasoning of classical theories. A supersaturated solution is assumed to contain spherical nuclei of radius  $R$  and with  $n_c$  particles, and the Gibbs free energy change on formation of these nuclei includes a term in the difference between the free energies of the solid and the liquid,  $\Delta\mu$ , and a term that represents

the surface free energy. In supersaturation conditions the first term is negative (drive towards the solid) and the second term is positive and responsible for the free energy activation barrier to nucleation:

$$\Delta G = 4/3\pi R^3 \rho_s \Delta\mu + 4\pi R^2 \gamma \quad (13.2)$$

where  $\rho_s$  is the particle density of the bulk solid, and  $\gamma$  is a surface free energy density. This function has a maximum  $\Delta G^*$  for a given  $R_{\text{crit}}$ , defining the size of the critical nucleus and also the probability of its formation, which is taken to be proportional to a Boltzmann-like factor in  $\Delta G^*$ . In addition to these thermodynamic factors, the theory includes some kinetic factors that take into account the obvious facts that (1) there must be a finite frequency of attachment for molecules docking onto the nucleus, and (2) the free energy barrier can be climbed from both sides. Using other simplifying assumptions, and simple geometrical factors for attachment, one ends up with the following expression for the nucleation rate per unit volume:

$$\text{rate} = (\Delta\mu/6\pi k_B n_c T)^{1/2} \rho_{\text{liq}} (24 D_s n_c^{2/3} / \lambda^2) \exp[-(16\pi/3 k_B T)(\gamma^3 / \rho_s \Delta\mu^2)] \quad (13.3)$$

$\lambda$  is a “typical” diffusion distance,  $D_s$  is the self-diffusion coefficient, and  $\rho_{\text{liq}}$  is the density of the liquid. Expressions of this kind have a rather unpleasant look and require funny numerical coefficients with lots of  $\pi$ s. More seriously, they are problematic because their overall reliability is the product of the reliability factors of all the embedded assumptions and approximations, a product that is nearly zero at the third assumption with 0.5 probability of being realistic. Models can be improved, phenomenological equations can be elaborated upon, densities can be taken as variable instead of constant, but one never gets past the basic stumbling points of a model, which is in all likelihood inadequate for the description of nucleation of crystals of complex organic molecules, for which the crucial quantities  $R$ ,  $\lambda$ , and  $\gamma$  are unknown or possibly even undefined.

There are other problems. Homogeneous nucleation, or nucleation in a continuous environment, is a tempting assumption in theorization [15], but known facts seem to indicate that it is just wishful thinking, at least for organic materials. Molecular aggregation is extremely sensitive to the presence of even minimal perturbing factors like tiny impurities or even cracks in the container’s surface, and every practicing chemist has experienced the effects of supplying mechanical energy by scratching the walls of a crystallization vessel. The sensitivity of nucleation processes to experimental, transient conditions is alarming from the standpoint of the construction of a unified theory of crystal nucleation. For example, stirring the melt has been reported to induce chiral symmetry breaking in the crystallization of 1,1'-binaphthyl [16].

At the other extreme, the formulation of molecular level theories is difficult if not impossible due to the intrinsic complexity of the molecular shape and potential in organic compounds. Molecular simulation studies of solid-liquid transformations concern mainly the Lennard-Jones fluid (the “spherical horse”), a hypothetical system

composed of spheres interacting by some sort of sphere-sphere empirical potential [17], or simple molecules like the alkanes, usually modeled in the united-atom approach (each methyl or methylene group being a single interaction site) [18], or small globular molecules [19].

As mentioned before, a single MD run through a melting process is not an equilibrium simulation. If a proper description of the equilibrium is desired, the simulation should be carried out a large number of times forwards and backwards through melting and crystallization – a fantastic task for even the most optimistic believer in the exponential growth of computing power. Alternatively, one may calculate the free energy of the crystal and of the liquid as a function of temperature, using free energy simulations (Section 9.7). One such calculation has been carried out for *n*-octane, using an all-atom model and allowing for the full flexibility of the chain [20]. The thermodynamic integration requires a reference state for which the free energy can be computed exactly: for the crystal, this is the so-called Einstein crystal, an ensemble of non-interacting particles each of which oscillates around its lattice site according to a given force constant, with total internal energy  $U_{\text{Ein}}$ ; for the liquid, the reference state is the ideal fluid at zero density, the ideal gas. An effective potential  $U_{\text{eff}}$  is then employed along with a step variable,  $\lambda$ , which carries the system from the reference state to the actual desired state. For the crystal, for example, one has:

$$U_{\text{eff}} = (1 - \lambda)U + \lambda U_{\text{Ein}} \quad (13.4)$$

$$\Delta F = F(\lambda = 0) - F(\lambda = 1) = - \int d\lambda < (dU_{\text{eff}}/d\lambda) > \quad (13.5)$$

A free energy difference becomes then an integral requiring only the knowledge of the internal energy  $U$ . The main problem of such approaches is that computing times scale with an unknown but for sure alarmingly high power of the number of atoms in the molecule, so the description of the molecule has to be restricted to a small number of sites and to very simple potentials. The return for such a huge computing investment rests on the accuracy of the potentials employed; for complex organic molecules where empirical force fields are often tentative and difficult to optimize, there are serious chances of using a big gun to shoot rubber bullets.

The ultimate challenge is a detailed description at a molecular level of the microscopic events that occur on the path from liquid to solid, both in structural and energetic aspects. In a brute force approach, one prepares a liquid computational box and applies standard molecular dynamics by lowering the temperature in steps, waiting for a crystallization trajectory to spring out of the computer. Success requires a big investment in time and effort, and a significant bit of luck, since MD trajectories are by definition unpredictable – if one wishes, chaotic, in the sense that small variations in initial conditions are unpredictably amplified as the simulation proceeds. The choice of temperature plays a crucial role, since too high a temperature may prevent molecules from sticking into place, and too low a temperature may deprive crystallizing molecules of the kinetic energy needed to swim through the liquid and reach their docking positions.

No wonder, successful studies of this kind can be counted on the fingers of one hand. An example is a much emphasized study of water freezing [21]: a computational box of 512 water molecules was simulated at 230 K, in “many” (one wonders exactly how many) trajectory calculations, each longer than  $1 \mu\text{s}$ , or a very long time for an MD simulation. During a time lag of about 200 ns, subsequent snapshots along the trajectory clearly show the formation of an hexagonal proto-structure of hydrogen bonds, followed by a formation of the complete hexagonal network typical of solid water.

In a different approach, free energy Monte Carlo calculations have been applied for the ice nucleation process through the “umbrella sampling” formalism [22]. In this procedure, the free energy is written as a function of some order parameters, connected with the geometry of the hydrogen bonding coordination sphere; the operator knows which values of these order parameters correspond to the solid and which to the liquid. The system is then “pulled” through phase space by a systematic variation of one or two of these order parameters, the leading parameters, while the free energy is minimized with respect to the others (the “lagging” parameters); in this way, a minimum free energy path is deliberately mapped for the nucleation process (in the same manner, umbrella sampling can be applied to any kind of chemical evolution, if the proper parameters can be chosen). The calculation reproduces the latent heat of melting of water, and estimates a free energy barrier to nucleation of 80 kT. Pre-crystallization nuclei are said to be dynamic in character, and the size of the critical nucleus is estimated at 210–260 molecules. These considerations and these numbers look like distant voices coming from an unexplored, far-away planet [23].

### 13.5 Vapor-liquid and vapor-solid equilibrium

The most striking news that one learns when studying vapor-liquid phenomena is that not only does the vapor need to nucleate a liquid droplet to condense, but that also the liquid needs to nucleate a gas bubble to evaporate [24]. On the theoretical side, the simulation is made easier because the vapor is relatively simple to handle, on the experimental side, vapor pressure measurements in vapor-liquid equilibrium are fairly easy to perform. The Gibbs ensemble Monte Carlo method (Section 9.8) can be applied to the vapor-liquid equilibrium with considerable success: vapor pressure curves, second virial coefficients, and other equilibrium properties can be calculated by molecular simulation, and, remarkably, good results can apparently be obtained by highly accurate *ab initio* quantum mechanical potentials [25a] or by simple empirical potentials [25b].

Crystal growth by sublimation is extensively used for obtaining high purity crystals. The nucleation and growth of crystals from the vapor invariably occurs by grafting to some solid support, usually in practice some cold spot on the walls of a container. A likely hypothesis is then that the solid surface somehow acts as a nucleation catalyst. In principle, nothing forbids the simulation of the vapor-solid equilibrium along the same lines as for vapor-liquid equilibria.

### 13.6 Glasses

“In the past few years the glass transition phenomenon has won general recognition as one of the outstanding unsolved problems in condensed matter physics” [26a]. These not exactly encouraging words appear at the top of a paper by one of the pioneers in the study of the glassy state. Glasses are solids without diffusional freedom but without long-range structural periodicity. To some extent, they can be assimilated to supercooled liquids, but in glass forming systems the viscosity has a sharp increase close to the so-called glass transition temperature until diffusion is entirely frozen out.

The glassy state can be induced by a rapid cooling of the liquid below the melting point; it is not known whether all substances must vitrify under given conditions, or only some substances with peculiar properties can be vitrified – and, if the latter is true, it is not known what these properties should be. An empirical rule states that the glass-forming ability of a molecular liquid is the ratio of the boiling point to melting point, which is generally above 2 for substances that vitrify easily [26b]; this ratio should reflect the sluggishness of the crystallization process due to poor packing efficiency. No wonder the rule has been questioned by the accumulation of more experimental data, as invariably happens with shape-aggregation relationships for organic compounds. The glassy state can be studied at varying temperature and pressure by many techniques, including thermal analysis and all methods that probe the relaxation times within the system, plus all usual spectroscopic techniques. The structure factor can be obtained by neutron scattering measurements, yielding radial density distribution curves (recall Section 5.8).

Two diagrams may be proposed to illustrate some of the basic properties of the glassy state: the heat capacity trace (thermogram) and the viscosity–temperature diagram. Schematic examples are shown in Figs. 13.5 and 13.6. The salient features of the thermogram, left to right, are: (1) there is a residual  $C_p$  difference between glass and crystal, showing that the glassy state has some extra energy “pockets”; (2) on heating, the glass goes through an endothermic bump that corresponds to some activated process for devitrification, followed by an exotherm that indicates evolution to a crystalline state; (3) after this, the crystal behaves in the usual manner and melts at the normal melting temperature. The viscosity diagram shows the difference between materials classified as “strong” where the plot is linear and follows an Arrhenius activation law:

$$\ln(\eta) = \ln(A) - (E^*/RT_g)(T_g/T) \quad (13.6)$$

and materials classified as “fragile”, where the viscosity breaks down much more sharply on increasing temperature, hence the name. These characteristic features must depend on the strength of the cohesion within the material, and, for example, hydrogen-bonding substances are usually “stronger” than “fragile” hydrocarbons, but exceptions are the rule in this kind of correlation.

There apparently is no doubt that the glass transition is reproducible, and hence can be discussed in thermodynamic terms rather than in evanescent kinetic terms.

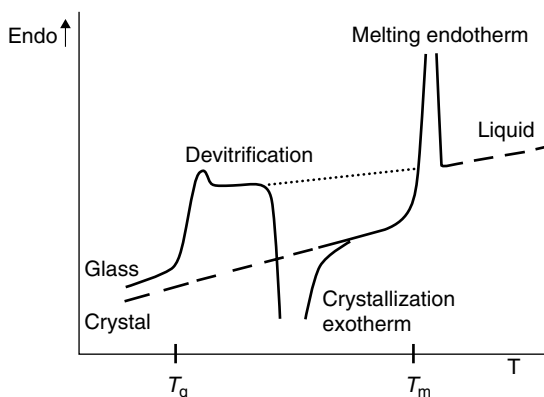


**Fig. 13.5.** Solid line: thermogram for the heating of a rapidly quenched liquid that has gone through the glass formation process. Dashed line: normal thermogram for the same material that has not gone through the vitrification process. Sample values for the glass transition temperature  $T_g$  and the melting temperature  $T_m$  are 117.5 and 178.15 for toluene. Adapted from ideas exposed in ref. [26].

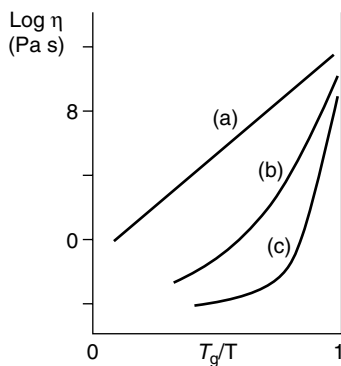


**Fig. 13.6.** Plots of viscosity against the glass transition to temperature ratio. Curve (a), “strong” material, Arrhenius law behavior; curves (b) and (c) increasingly “fragile” materials, where internal breakdown occurs as soon as temperature rises above  $T_g$ .

But what is the level of molecular organization within the glassy state? There certainly is a short range association effect quite similar to that observed in normal liquids, observable by peaks in the radial distribution functions, which reflects the main intermolecular bonding abilities of the compound; for example, some structuring arises from interactions between aromatic rings in benzene derivatives, or typically by hydrogen bonding. Depending on the strength of the intermolecular cohesion, there may also be some intermediate range ordering, possible due to a structuring among

clusters of molecules, rather than among molecules themselves, which is revealed by a “pre-peak” in the static structure factor at very short  $\theta$  or distances of 10–30 Å, as measured by neutron scattering [26,27].

The temperature and pressure evolution of glass-forming systems can be modeled by evolutionary molecular simulations like Monte Carlo or molecular dynamics. A good sample case is *m*-toluidine (1-methyl-3-aminobenzene), which has been extensively studied by a combination of neutron scattering and Monte Carlo simulation [27]. An analysis of the temperature, pressure, and isotopic substitution dependence allows an assignment and tentative rationalization of the features in the static structure factor: those features which depend on pressure are ascribed to the exclusion volume of the aromatic rings (a repulsive effect) while temperature-dependent features are associated with bond stretching phenomena, ideally hydrogen bonding. The pre-peak intensity increases on lowering the temperature down to the glassy state: interpreted as due to clustering phenomena induced by hydrogen bonding, this intermediate-range order introduces a fascinating, but disturbing, character of at least partial structural inhomogeneity into the glassy state and, possibly, into supercooled liquids in general [28]. A more detailed analysis [29] using molecular dynamics simulation allows a breakdown of the structure factor intensities over separate atomic contributions: it shows that the pre-peak results mainly from the contributions of nitrogen atoms involved in hydrogen-bonded molecular clusters. In addition, the simulation mimics almost perfectly the  $C_p$  anomaly at the glass transition (Fig. 13.7) and allows a molecular level interpretation of the structural rearrangement at the transition temperature, which involves a change in the reciprocal orientation between hydrogen bonds and inter-ring interactions. This example illustrates the efficiency and the richness of microscopic detail afforded by accurate molecular simulation in the analysis and interpretation of experimental observations – it goes without saying that the simulations also perfectly reproduce all the properties of the corresponding normal liquid.

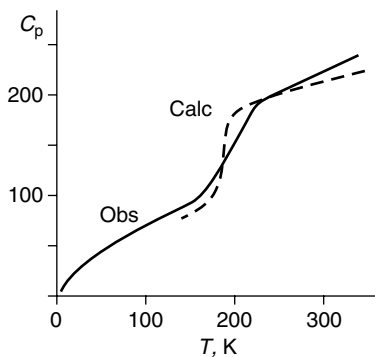


**Fig. 13.7.** Simulated (dashed, from ref. [29]) and experimental (full line, from ref. [26b]) evolution of the heat capacity of liquid toluidine through the glass transition. The agreement is impressive.

### 13.7 Liquid crystals

This beautiful oxymoron refers to a particular state of matter, encountered with organic compounds whose overall envelope presents a particularly simple shape, most often an ellipsoid or a discoid. These molecules organize themselves with a varying degree of structural periodicity (order), in one or two dimensions, intermediate between the liquid and the crystal, hence the name of mesophases and mesogenic compounds. Since the structural periodicity is to some extent commensurate with the molecular shape, the orientation of the elongation axis or of the main plane are easily recognizable geometric descriptors of the intermolecular structure of these particular condensed phases. The preparation of mesogenic compounds and the experimental analysis of the corresponding phases are the subject of entire books in themselves and will not be reviewed here. The same applies to the evolutionary simulation of mesophases [30]; only a flavor of these simulations will be given here.

Although the complete atomistic simulation of ensembles of mesogenic molecules is within reach of present computational facilities, the traditional treatment of liquid crystals in molecular dynamics or Monte Carlo simulations makes use of the Gay–Berne potential, an ingenious computational machine whose aspects deserve to be described here for their epistemological implications. An ordinary Lennard-Jones (LJ) potential, equation 4.38 or 4.40, can be written as a function of the distance between two particles,  $R_{ij}$ , the well depth  $\varepsilon$  and the equilibrium separation  $\sigma$ . An ellipsoidal object is identified by the position of its centroid and by an orientation unit vector  $\mathbf{u}$ , and the Gay–Berne (GB) potential is a modified LJ that takes into account the anisotropy of the ellipsoid, both in energy and equilibrium separation:

$$\text{LJ:} \quad U_{\text{LJ}} = U(R_{ij}, \varepsilon, \sigma) \quad (= 4.38) \quad (13.7)$$

$$\text{GB:} \quad U_{\text{GB}} = U[R_{ij}, \varepsilon(\mathbf{u}_i, \mathbf{u}_j, R_{ij}), \sigma(\mathbf{u}_i, \mathbf{u}_j, R_{ij}), \mu, \nu] \quad (13.8)$$

In the above formulation  $R_{ij}$  is the distance between centroids, while the overall distance dependence is still of the 12-6 type. Both well depth and equilibrium separation depend on the distance and relative orientation of the two ellipsoids, and two extra parameters,  $\mu$  and  $\nu$ , add flexibility to the model by exponential scaling of the implied dot products between orientation vectors. All in all, a GB potential depends on four parameters, the length/breadth ratios for  $\varepsilon$  and  $\sigma$ , plus  $\mu$  and  $\nu$ . Figure 13.8 shows the nice result: an orientation dependence of the potential. In addition, the ellipsoids or the discoids can be made electrically active by imposing some central multipoles along the molecular envelope; the calculation of the multipole energy then is easily accomplished by standard electrostatic formulas (see Section 4.2 and ref. [30]). For two dipoles  $\mathbf{d}_i$  and  $\mathbf{d}_j$  at a distance  $\mathbf{R}$ , for example, the total simulation energy of the liquid crystalline sample then becomes:

$$U(\text{dipole}) = (d_i d_j / R^3) [\mathbf{d}_i \cdot \mathbf{d}_j - 3(\mathbf{d}_i \cdot \mathbf{R})(\mathbf{d}_j \cdot \mathbf{R})] \quad (13.9)$$

$$E_{\text{TOT}} = U_{\text{GB}} + U(\text{dipole}) \quad (13.10)$$

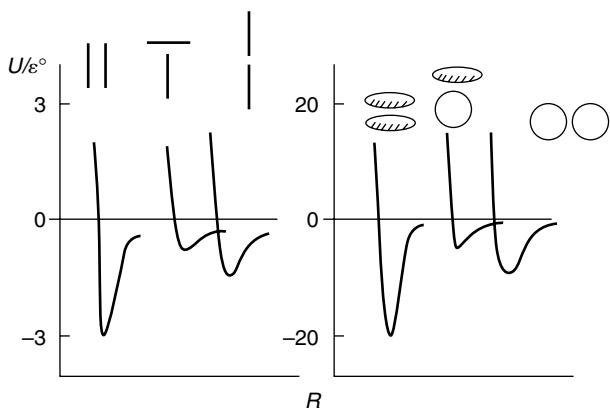


**Fig. 13.8.** Gay-Berne potentials: limiting cases of reciprocal orientation between ellipsoids or discoids.  $\varepsilon^\circ$  is a reference well depth. In discotics, the length/breadth ratio is substituted by a thickness/diameter ratio. Adapted (with permission) from ref. [30].

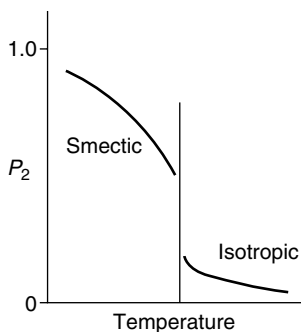


**Fig. 13.9.** Typical result of a simulation for a liquid crystalline ensemble: as the clearing temperature is reached, the order parameter  $P_2$ , equation 13.11, suddenly drops to zero.

In standard modeling, the parameters of the force field are optimized to reproduce experimental properties of real substances, e.g. heats of sublimation or of melting, and the parametric force field is then used to predict unknown values of the same and other physical quantities. In the study of liquid crystals by the above formalism the logical path is sometimes different: one asks for certain properties, and then tries to find the parameters that would be needed to produce such a result. Consider, for example, the clearing point between a smectic phase and the liquid; the transition is easily characterized by the evolution in temperature of the second moment of the distribution of molecular orientation vector  $\mathbf{u}$  with respect to a principal direction  $\mathbf{e}$  [30]:

$$P_2 = \frac{3}{2} \langle (\mathbf{u} \cdot \mathbf{e})^2 \rangle - \frac{1}{2} \quad (13.11)$$

A schematic illustration of this situation is shown in Figure 13.9. Clearly the position of the clearing point is tunable according to the values assigned to the parameters in the GB potential and to the molecular multipoles. The properties of the real molecule that would exhibit the required property are then inferred from the values of the parameters, e.g. a certain length/breadth ratio and certain values of the molecular multipoles.

### 13.8 Nucleation and growth from solution: Experiments

To many people, chemistry is a science of colors; a typically impressive experiment carried out by elementary school teachers is the mixing of two colorless solutions to obtain a colored product. It is easy to understand how awe-inspiring it can be, along the same line, the mixing of two transparent solutions to yield a turbid medium, or the precipitation of solid matter with a clearly distinguishable external morphology, faces, and dihedrals [31]. This is as close to a miracle as the fantasy of the layman can go, and there is no doubt that crystallization has exerted a special fascination throughout the centuries, with the birth and spread of crystal fads, some of which survive today in the selling of healing crystals, miracle pyramids, and the like. It must be said that the precipitation of a nice and clean crystalline material perhaps after a long synthetic effort is a source of special satisfaction and reward even to an experienced chemist [32], just as the stubborn refusal of some solutes to coagulate into their solids is a source of frustration and a major obstacle to further purification.

#### 13.8.1 Overview

The basic tenets of the science of crystal development from solution are few and very broad: (1) solute molecules associate in solution until the newly formed aggregate grows to a certain size; this stage is usually called “nucleation”; (2) some of the associative nuclei then further develop into larger crystals; this stage is usually called “growth” – but notice that the verb “to grow” had also to be used in the definition of nucleation.

In macroscopic phenomenological terms, the formation of an elementary aggregate involves a change in free energy due to aggregation itself, and a change in free energy due to interface tensions, as already outlined in equation 13.2. The development of the theory of nucleation from solution follows a path that is very similar to that for nucleation from the melt, with the obvious additional complication that the system is now a two-component (if not a many-component) one. However, as soon as the nucleation heterogeneity appears, the basic concepts of thermodynamics are put in question. In fact, free energy must be a state function, but in a heterogeneous system the state-defining variables may not be just the traditional ones, temperature, pressure, volume, chemical compositions, but must be supplemented by some descriptor of the amount of heterogeneity (order? size distribution?), and the recognition and measurement of these supplementary variables is nearly always extremely difficult,

because very few if any of the traditional chemical analysis techniques can be made sensitive enough to probe the intimate structure of these microscopic and fluctuating aggregates. Especially for large and flexible organic molecules, the very concept of phase equilibrium becomes questionable as most of the time the experimental reproducibility and identification of states and phases are difficult and one does not know, literally, what state or phase one is speaking of.

Then the nuclei grow into macroscopic crystals, but there is no way of properly defining a transition from the nucleation to the growth stage. There is no doubt that the growth mechanics must be directed by the template provided by the pre-existing stable structure of the nuclei. Phenomenological theories of crystal growth use schematic models of the growing surfaces, which are postulated to be very flat and regular at low temperatures and to become “rough” at higher temperature; this roughening is due to the presence of kinks, steps, and ledges, whose efficiency in promoting growth is evident on the basis of simple geometrical intuition, because a molecule attached at a kink site interacts with the bulk in two or three directions, while a molecule on a flat surface interacts along one direction only. Again, while working reasonably well for simple particles, such models are clearly inadequate to treat complex molecules. Given such premises, it is not surprising to learn that nucleation and growth theories for real organic molecules are presently in an unsatisfactory state.

Nucleation, growth, and transformations among nucleating and growing species have been and are being studied extensively, taking full advantage of the recent large improvements in analytical techniques. The overview is at the same time an extremely stimulating and outrightly frustrating one: the dynamics of these processes is seen to depend on nearly anything: temperature, chemical nature of the solvent, solute solubility, pH, stirring rate, total volume of the sample [33]; chemical additives (and hence impurities in nanoconcentrations) [34]; sonication (treatment with ultrasonic waves) [35]; confinement in microporous solids, emulsification [36]; epitaxy [37], and even cross-fertilization of various polymorphic nuclei [38]. Apparently, an external electric field or the extent and direction of polarization of an external light source can influence in stereoselective ways the nucleation and crystallization of highly polarized molecules [39].

### 13.8.2 *Light scattering, calorimetry*

So the hunt for this elusive entity, the growing nucleus, is open. Useful analytical techniques for the study of crystal nucleation and growth must be sensitive to the size of the evolving clusters, and, ideally, also to the detailed intermolecular structure of these clusters. The first requirement seems more within reach than the second.

When aggregates grow, the solution becomes turbid because of light scattering, and accurate measurements of the photon autocorrelation function provide a direct access to the radius of the scattering nuclei. This technique can be comfortably used for large nuclei formed by crystallizing protein molecules: in a typical study on lysozyme [40], cluster radii were seen to grow from 20 to 50 Å in about one hour,

with the number of different clusters decreasing from 1000 to 10 over the same period. For ordinary organic molecules, practical difficulties arise when using this technique, due to the smallness of the clusters, to multiple scattering, and to the requirement that the suspension be of non-interacting monodisperse clusters (all nuclei of the same size). Nevertheless, light scattering techniques are employed to study the formation of liquid droplets from water vapor [41], allowing the measurement of nucleation rates (number of nuclei formed per unit of volume and time) and of cluster composition, which for water range from  $10^5$  to  $10^9 \text{ cm}^{-3} \text{ s}^{-1}$ , and from 20 to 30 molecules per cluster, respectively.

Similarly, the particle size and number concentration in crystallizing systems can be counted directly through the obscuration of a laser beam by particles flowing between the beam and a photodiode [42], or via the attenuation of a sound wave traveling through the system [43], with the added advantage in the latter case that the measurement is not hampered by optical saturation. Treating the experimental data by classical nucleation theories, nucleation and growth rates can be obtained, with orders of magnitude of  $10^{12} \text{ m}^{-3} \text{ s}^{-1}$  and  $10^8 \text{ m s}^{-1}$ , respectively. Particle sizes, apparently, can vary from 5 [42] (a puzzling, astonishingly small number) to 500 [43].

In an alternative to counting the number of condensed particles, one can try to monitor the concentration of remaining solute [44], or some other thermodynamic property that evolves with cluster formation: for example, microcalorimetry can measure the heat absorbed as crystallization occurs, and thus can draw a de-supersaturation curve [45]. Needless to say, none of the above directly or indirectly touches upon the question of the internal structure of the generated clusters.

### 13.8.3 *Chemical spectroscopy*

Why not use standard chemical spectroscopy to study intermolecular association and nucleation? The main obstacles are (1) that one must find signals that change upon association, and this is not easy within the weak force regime proper of intermolecular bonding, except perhaps for hydrogen bonds, and (2) that one must also have a clear dependence on cluster size, which is even more difficult to achieve, with the added complication that (3) many clusters of different size may be present in the nucleating solution. For example, the existence of hydrogen-bonded aggregates of the size of a few molecules could be ascertained in the benzyl alcohol–carbon tetrachloride system [46], but only by a multivariate analysis of an entire spectral region ( $3,100\text{--}3,700 \text{ cm}^{-1}$ ), because there is no obvious way of clearly separating signals from monomers and from oligomers. In a similar manner, a principal component analysis (recall Section 8.10.2) of the  $1,600\text{--}1,680 \text{ cm}^{-1}$  spectral region carried out on a crystallizing progesterone solution could distinguish between spectral features of the solute in solution and the solute crystals [47], and Raman spectroscopy can distinguish the relative amounts of two polymorphic phases in a polymorphic transformation by quantitative calibration of peak heights over the whole  $200\text{--}1400 \text{ cm}^{-1}$  region [48]. A subtle change in spectral features in the carbonyl absorption region

between tetrolic acid in chloroform and in dioxane spots the formation of a heterogeneous hydrogen bond that leads to the crystallization of a dioxane solvate [49]. Here we are here close enough to gleaning what molecules are doing in solution prior to the crystallization event.

NMR spectroscopy is another obvious candidate: if, after all, it is possible to determine the structures of proteins in solution, why should it not be possible to determine the structure of aggregating molecules? In a relatively straightforward experiment, the disappearance of monomeric lysozyme macromolecules from solution after supersaturation was recorded [50], but for small-molecule clusters, the problem is always the same; scarce structural sensitivity. In a test study, the NMR spectra of dimerizing amide compounds were analyzed in terms of the formation of dimers and chains, by varying the solute concentration to find association-dependent bands [51]. A correlation between dimer structures found in solution or found in the crystal by X-ray diffraction was found, again, opening a window on solution behavior, possibly on the way to more complete association studies, although even here the determinations had to rely on chemical shift changes as small as 0.1–0.2 ppm or even less. One cannot imagine what should be measured for weakly bound van der Waals complexes.

#### 13.8.4 *X-ray scattering and diffraction*

The routine availability of high-power synchrotron radiation is likely to play a major role in the development of in situ analysis of the nucleation event. The high-brilliance, entirely wavelength-tunable radiation can probe particle sizes in the 30–1000 Å range by scattering, or in favorable cases even the ordering at atomic level within the clusters, in the 2–10 Å range, just as in ordinary powder diffraction experiments. The high output radiation intensity allows data collection on the timescale of milliseconds and thus permits time-resolved crystallization studies. The nucleation of glycine was studied by X-ray scattering [52]: the relationship between scattered intensity and particle radii and shape goes through a phenomenological model involving fractals, which, if rather obscure to the chemist, is apparently reliable enough to draw vital conclusions about the nucleation mechanism: glycine exists in solution as a mixture of monomers and dimers, which at increasing supersaturation coalesce into liquid-like particles, which then reorganize into crystalline entities. These conclusions are enough to dispose in one single stroke of classical nucleation theory which proceeds from differences in chemical potential between solution and crystal.

In diffraction experiments, the diffraction pattern is directly obtained from the crystallizing supersaturated solution, and when the contribution from the diffuse scattering due to the solvent is filtered out, the data allow a time-resolved study of crystal formation. Solution patterns can be compared with the pattern from dry powders, and the growth process can be monitored; for example, a nice coincidence of solution and dry powder diffraction patterns was observed for benzamide and dibromoaniline [53]. Such techniques are widely used in nucleation and growth studies for inorganic materials [54].

### 13.9 Crystal growth and morphology

The morphology of minerals and inorganic crystals is usually evident, and is actually impressive, as one may realize by thinking of gems. The strong forces, mainly of coulombic nature, that hold together these materials impart to them a strong mechanical resistance and a strong anisotropy. Growing single crystals of weakly bound organic materials is much more problematic: samples are usually very small, and their outer morphology is much less well defined or recognizable. For an impression of actual morphology considerations in the field of organic crystals, Table 13.1 collects the recorded qualifiers of sample shape in a large set of crystal structures in the Cambridge Structural Database; these qualifiers are perforce approximate, if one recalls that samples for X-ray analysis may be as small as fractions of a millimeter, but nonetheless one can see there a predominance of growth forms that lead to an overall globular shape, rather than plate or acicular. The sampling is not unbiased because it refers to crystals selected for X-ray analysis, and an expert crystallographer will always select for that purpose an individual as similar as possible to a sphere, even when the crystal batch contains individuals of different morphologies.

#### 13.9.1 *Crystal faces, attachments energies, and morphology prediction*

After the early nucleation and accretion events, large aggregates of unmistakable crystalline nature eventually result, and further attachment of molecules from a surrounding fluid phase leads to what is known as crystal growth proper, an intrinsically epitaxial, two-dimensional phenomenon occurring on well-developed crystal faces,

**Table 13.1** Number of qualifiers of crystal morphology in the Z(1) database (see Chapter 8): 8,519 total entries. 3D, 2D, and 1D approximately label crystals grown in globular, plate or acicular form, respectively.

Descriptor	
Prism	2946
Block	1343
Parallelepiped	238
Cube, box	140
Total 3D	55%
Plate	1546
Slab	43
Total 2D	19%
Needle	1169
Cylinder, rod	226
Total 1D	16%

as opposed to the three-dimensional shaping of previous aggregates, which can be either in crystalline, liquid, or semi-structured states.

Each face of a macroscopic crystal must be parallel to a Bragg ( $hkl$ ) plane (see Fig. 5.13); when cell parameters are known, it is a relatively easy matter to assign Bragg indices to each prominent face observed on a macroscopic crystal sample, and vice versa. Early crystallography used planes and angles between them to determine cell parameters – at least, when large enough crystals for visual observation can be grown. If the crystal structure has been determined by X-ray diffraction, an appropriate projection can be performed so as to have a view of the internal crystal structure down the perpendicular to each face. What, then, should one “see” on a given ( $hkl$ ) face? It is important to realize from the very beginning that the surface population on a given face can be uniquely defined only in terms of lattice points; but when considering the actual molecular structure with its electron density envelope, and the organization of matter around lattice points, including the symmetry operations within the cell, what one “sees” depends on where one “cuts” (Fig. 13.10). In other words, a static definition of surfaces and slices through the crystal structure, a vital link between macroscopic morphology and molecular level structure on the way to the molecular modeling of surface properties, depends on some subjective choices. For simple cubic crystals made of atomic spheres (again, the “spherical horse”) things may be easier, because atomic positions mostly coincide with lattice points, and surfaces can be classified as compact, flat, or rough. For organic crystals made of complex, flexible molecules, these definitions lose much of their uniqueness.

On the other hand, Fig. 13.11 shows a sketch of the actual situation at the boundary between the growing crystal face and the solution. Solute molecules approach the surface in conformational freedom, amidst solvent molecules, some of which are also adsorbed on the crystal surface. There is little doubt that the structure of the bulk solution is different from that of the solution close to the surface, which limits molecular mobility and induces an electrostatic potential onto the solute molecules,

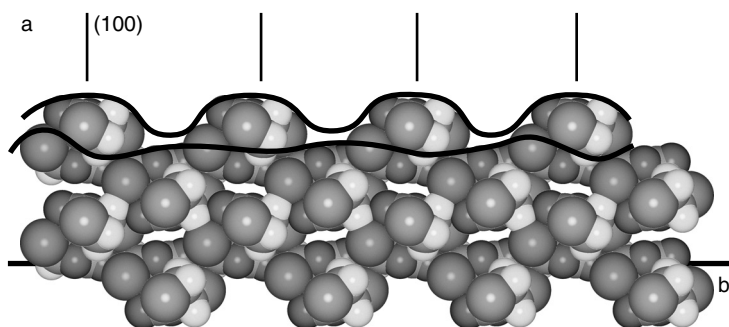


**Fig. 13.10.** Shows a cut perpendicular to the  $a$  direction (perpendicular to the plane of the page): the two wavy lines correspond to a different choice of surface molecules, and hence to a different surface structure, roughness, etc.

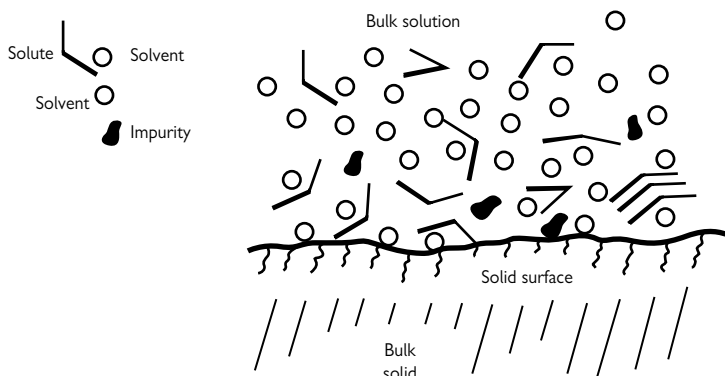


**Fig. 13.11.** A schematic representation of the complex situation near a crystal–solution interface. Shows solute molecules with variable conformation in the bulk solution, partial structuring of solute molecules near the interface, and solute, solvent and impurity particles adsorbed on the solid surface. The structure of the solid at the surface may be different from the bulk solid structure.

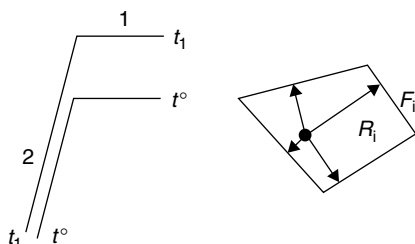


**Fig. 13.12.** Left: explanation of the relative growth of two faces: between time  $t^{\circ}$  and  $t_1$ , surface 1 is displaced (grows) faster, surface 2 grows more slowly, so that at time  $t_1$  surface 2 has become much larger than surface 1. Right: the construction of morphology, shown in two dimensions: the lengths of vectors  $R_i$  out of a selected origin (black circle) are proportional to the growth rate, and the external morphology results from the envelope of faces  $F_i$  perpendicular to these vectors.

and hence is likely to induce a partial solute structuring. Impurities also play a substantial although hardly predictable role, being active at a level of the order of  $10^{-9}$  M [55]. The solid itself is likely to be sensitive to the presence of the fluid phase, with a partially reconstructed surface structure that may differ from the bulk structure. As the crystal grows, the addition of new molecules to the various possible faces occurs in a highly anisotropic fashion, because the energetic path to attachment is obviously different for different surface aspects. As a result, some faces grow faster than others, and the macroscopic specimen takes up its experimental morphology, as explained schematically in Fig. 13.12.

With a simple construction, the predicted crystal morphology is established as explained in Fig. 13.12 (right), using expansion vectors whose direction is determined

by the face indices and whose modulus depends on the growth rate. The question is, how does growth rate depend on surface structure? Early phenomenological theories assume flat surfaces in the first place, which grow only by virtue of molecular attachment to some dislocation. Along these lines, the growth rates may be taken just as inversely proportional to the  $d(hkl)$  spacing (Fig. 5.13); the smaller the spacing, the stronger the cohesion; or, in a more appropriate way, as proportional to the attachment energy, which is the energy released when a new layer of molecules is deposited on the surface. The attachment energy can be calculated by systematically removing surface molecules, although with some reference-dependent assumption, as discussed above, and computing the related energies by atom–atom empirical potentials. In this way, computer programs for the tentative prediction of crystal morphology can be set up [56].

As a help in the identification of the relevant surface networks, the periodic bond chain concept is sometimes used: a molecule within the network is represented by a point, and the network is kept together by “bonds” that are, in essence, molecule–molecule energies calculated by the applied intermolecular potentials [57] (see the “structure fingerprints” of Section 14.2.3). On such flat surfaces, the molecules are assumed to be closely packed in regular arrays more or less like spheres, until some external event (typically, a rise in temperature) induces a so called “roughening” transition, or the creation of non-specified surface irregularities that create molecular niches into which the incoming molecules may dock more promptly. If one considers the complex structure of a molecular surface (Fig. 13.10), it is doubtful that such simplified schemes may lead to a consistent routine prediction of crystal morphology. They may perhaps be applied more confidently to the prediction of crystal growth by sublimation, where the complications due to the presence of the solvent are removed.

The simulation of morphology using attachment energies only is static in nature. As an improvement, in an attempt to include surface roughening, the Monte Carlo method is used for the simulation of the attachment process over the crystal graph, to fill the gap due to the neglect of the effects of supersaturation and temperature; differently from free atomistic simulation, however, in this approach a number of kinetic and thermodynamic constraints (crystal network, supersaturation and kinetic parameter) are input to and enforced throughout the calculation [58]. Not surprisingly, while static attachment methods show little sensitivity to the force field employed, the Monte Carlo approach is extremely sensitive to small variations in the force field, due to the stochastic nature of the phenomenon and to the importance of molecular detail in the anisotropy of surface roughness. In an extensive comparative predictive study of paracetamol morphology, different results were obtained with Dreiding, distributed multipole and Compass force fields (see Chapter 2), none of which gave good agreement with the experimental morphology [59]. One sees here a harbinger of the complex interplay between the scope of the simulation method and the accuracy of the force field that also appears when dealing with crystal structure prediction (Section 14.4).

Crystal morphology is well known to be extremely solvent-dependent. If predictions other than in vacuo are desired, the influence of the solvent must be taken into

account, and the simplest way of doing this is to consider an effective attachment energy,  $E^*(\text{att}) = E(\text{att, vacuo}) - E(\text{att, solv})$ , where  $E(\text{att, solv})$  is the energy cost for removing the solvent from the surface. This quantity can be obtained by molecular dynamics simulations in which a crystal surface is equilibrated in the presence of a solvent layer, and by partitioning the total configurational energy into crystal–crystal, solvent–solvent and crystal–solvent terms, or by appropriate manipulations of the total energies of the separate crystal and liquid phases against the energy of the heterogenous system. The modified attachment energy  $E^*(\text{att})$  is then introduced in the usual static scheme for the prediction of the crystal morphology [60].

### 13.9.2 *Electron micrography and atomic force microscopy (AFM)*

Well grown faces of organic crystals can be studied in some favorable cases by ordinary optical microscopy, to a detail of perhaps some fractions of a millimeter. For higher resolution, use is made of electron micrography, an imaging technique that relies upon the interaction of an electron beam with the electron density of the surface atoms. Atomic level resolution can be obtained by the atomic force microscope, a unique tool for revealing molecular and atomic detail on surfaces. Its setup (Fig. 13.13) relies on atomic level technology but is disarmingly simple in concept. A sensing probe, consisting of a tip made of an inert material (e.g. SiN) about 100 Å or less in diameter protrudes from the end of a flexible cantilever, and is brought at atomic distance from the surface to be explored by a piezoelectric actuator ( $z$ -actuator). The tip interacts with the surface and is pulled by the intermolecular force; as the surface is moved below the tip by  $x$ – $y$  piezoelectric actuators, the  $z$ -actuator moves the tip up and down to maintain a constant force between the surface and the tip. These up and down movements are translated into angular deflections of a laser beam reflected off the end of the cantilever towards a photodetector. The response of the photodetector is converted to a topographical image of the surface by image processing techniques. The dimensions of the apparatus are amazing – the tip–surface distance is of the

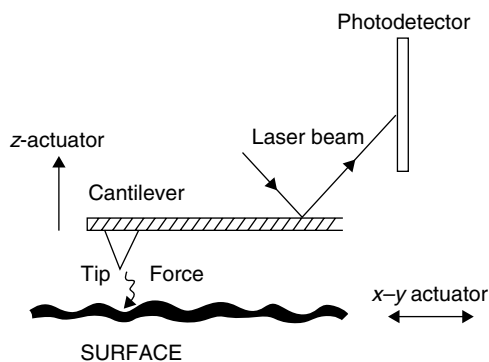


**Fig. 13.13.** Schematic drawing of an AFM instrument.

order of 2 Å, the cantilever spring constant is of the order of  $0.1 \text{ N m}^{-1}$ , and actuators work at the rate of 1 Å displacement per volt. The images thus obtained have a captivatingly realistic appearance, showing hills and valleys of atomic dimensions. One should never forget, however, that what one is actually seeing is not really nuclei and electrons, but a reconstructed image of up and down cantilever displacements for constant-force condition. AFM can be applied to non-conducting materials, differently from STM (scanning tunneling microscopy), and, even more important for the structural chemistry of crystal formation, it can be applied to surfaces immersed in a solvent and under solvent flow conditions, so that the degree of saturation of the solution can be controlled [61].

AFM probes a crystal surface of nanoscopic dimensions at an advanced stage of crystallinity, and hence is the ideal tool for studying crystal growth and dissolution. The list of phenomena that can be studied by in situ AFM on organic crystals in solution is long and is limited only by the investigator's imagination: surface topography, dissolution and growth of faces, advancement of growth terraces; etching by different solvents; the effect of different degrees of saturation or of additives; epitaxial growth; and all these phenomena can be fairly easily correlated with the surface structure at atomic resolution, if known by X-ray diffraction on single crystals. In addition, the results of AFM experiments can be compared with and supplemented by the results of static or dynamic simulations of attachment energies or of the actual crystal-liquid interface.

### 13.10 Evolutionary molecular simulation

There is little hope of studying theoretically the complex intermolecular situation sketched in Fig. 13.11 with even modest accuracy, unless evolutionary molecular simulation is employed. Recourse is thus made to the classical arsenal of such simulations, broadly subdivided into Monte Carlo (MC) and Molecular Dynamics (MD). The conceptual foundations of these two methods, and their computational feasibility, are now reviewed again from the perspective of their use for nucleation and growth studies.

In MD, time is a clearly singled out variable in a deterministic simulation based on a postulated force field and on the classical equations of motion. For the simulation of an evolving crystal aggregate, MD has the obvious advantage that the kinetics of the process is transparent, as accretion rates can be immediately described as a function of computational time, although the rate of any molecular process is obviously dependent on the postulated force model. In contrast, there is no apparent time variable in an MC simulation, because evolution steps are random and may randomly affect molecular evolutions which in reality happen on different timescales. If, as is often the case, time in MC is taken as proportional to the number of moves, one is implicitly assuming that all molecular moves occur on the same timescale, perhaps not a very severe approximation in studies of molecular aggregates bound by nearly isotropic van der Waals forces. In a variant of the MC formulation, called kinetic Monte Carlo (KMC)

[62], moves are accepted or rejected according to a comparison between a random number  $0 < r < 1$ , and a probability of the performed move, estimated according to preselected rate rules; compare this criterion with the standard MC energy criterion of equation 9.10b. The time spacing between successive MC moves is thus calculable, but only at the price of having to formulate sensible rate rules.

MD simulations of crystal growth can be readily set up, at least in principle. One may think of using a computational box made of a crystal slab in contact with a liquid phase; this would have the obvious problem that at any non-zero temperature part of the solvent would be lost to the overhanging vacuum, and that the crystal slab surrounded by vacuum would distort under the action of extreme surface forces. These problems may be avoided by periodic boundary conditions, using a computational box in which a crystalline lamella is enclosed between two solvent slabs so that on applying the periodicity conditions, the continuity of the two phases is preserved. The MD approach has the usual shortcomings: the first is the timescale problem, which is especially acute in this case because nucleation and growth occur on the scale of seconds, at the shortest, while MD simulation may last milliseconds at best. Put another way, typical nucleation rates may be of the order of the appearance of one particle every  $10^{14}$  seconds in a cube with a side of  $10 \text{ \AA}$ . The second is the size problem, because  $10^3$ – $10^4$  molecules are considered instead of  $10^{23}$ . Such simulations are therefore restricted to the study of some elementary events in the nucleation or growth path, such as instantaneous attachment or detachment of solute and solvent particles, or the different structuring of solvent layers close to or far from the crystal surface [63]. Alternatively, extreme supersaturations must be used, to convince solute molecules to aggregate out of the solution, with the obvious consequence that calculated nucleation rates may be fourteen orders of magnitude larger than experimental ones [64]. Better results are obtained with small, globular and rigid molecules such as  $\text{SeF}_6$  [65], or when the aggregation forces are very strong, as for covalent C–C bonds [66].

Both in MD and in MC, long simulation periods are spent in observing evolutions that are irrelevant to the process under study, such as internal molecular vibrations, or small amplitude oscillations around molecular positions in the liquid, while the process-driving steps like, for example, diffusion from the solute to the crystal surface, occur very seldom over extremely large numbers of MC moves or MD steps. In this respect, MC has an advantage over MD because in MC a “move” can be anything the operators want it to be, provided that reasonable acceptance criteria are selected. Thus, one has MC “smart move” [67], in which the smart moves are the change of identity between a solute and a solvent particle, or the swapping of the position of a solute and a solvent molecule in close contact. These smart moves greatly enhance the essential transport phenomena in the computational box. In the so-called aggregation-volume-bias variant of the Monte Carlo scheme, [68] the computational box space is explicitly divided into aggregating and non-aggregating zones, and MC moves are swaps between the two zones; in essence, the particle is “picked up” from a bulk solution region and “stuck” into an aggregating zone, thus elegantly straddling the long and uncertain diffusion path that would result from the usual Metropolis-type

MC in which moves are only as described in equation 9.10. In MD, umbrella sampling can be used to drive the system to the desired path through configurational space.

### References and Notes to Chapter 13

- [1] Westwell, M. S.; Searle, M. S.; Williams, D. H. The “*n*” effect in molecular recognition, *J. Mol. Recognition* 1996, **9**, 88–94. The title of this paper stems from an analysis of the sharpness of the melting transition, in spite of the flatness of the free energy landscape (free energy changes in the surroundings of the equilibrium point are very small: for water, for  $\Delta T = 10$  K from equilibrium  $\Delta G_{\text{melt}}$  is only  $0.2 \text{ kJ mol}^{-1}$ ). The root of the problem is in the effects of size and of cooperativity in extended arrays of weak interactions.
- [2] Dannenfelser, R. M.; Surendran, N.; Yalkowsky, S. H. Molecular symmetry and related properties, in *SAR and QSAR in Environmental Research*, 1993, Vol. 1, pp. 273–292, Gordon and Breach. This paper includes a large collection of melting entropies.
- [3] For a more detailed discussion see Pinal, R. Effect of molecular symmetry on melting temperature and solubility, *Org. Biomol. Chem.* 2004, **2**, 2692–2599. This paper also gives the formal connection between melting entropy and ideal solubility.
- [4] See Gavezzotti, A. Molecular symmetry, melting temperatures and melting enthalpies of substituted benzenes and naphthalenes, *J. Chem. Soc. Perkin 2* 1995, 1399–1404. This paper apparently shows that the effect is at work also for asymmetrically substituted compounds, so the relationship to symmetry number becomes less strict, and that more symmetric molecules also have higher melting enthalpies. Recall also Section 1.4. See also Brown, R. J. C.; Brown, R. F. C. Melting point and molecular symmetry, *J. Chem. Ed.* 2000, **77**, 724–731, quoting an original statement by Thomas Carnelley (1882) more or less to the same effect: “of two or more isomeric compounds, those whose atoms are more symmetrically or more compactly arranged melt higher...”. A related paper is Yu, L. Inferring thermodynamic stability relationships of polymorphs from melting data. *J. Pharm. Sci.* 1995, **84**, 966–974.
- [5] Reuter, J.; Buesing, D.; Tamarit, J. L.; Würflinger, A. High-pressure differential thermal analysis of the phase behavior in some *tert*-butyl compounds, *J. Mater. Chem.* 1997, **7**, 41–46. This paper also discusses some phenomenological theories of crystal melting (like the Pople-Karasz theory, 1961) that take into account orientational disorder in the solid, based on ideas presented in 1939 by Lennard-Jones and Devonshire. The essential parameter of such a theory is the ratio of the barriers to reorientation and to diffusion, which is also a measure for the anisotropy in molecular shape.
- [6] (a) Gavezzotti, A. A molecular dynamics view of some kinetic and structural aspects of melting in the acetic acid crystal, *J. Mol. Struct.* 1999, **486**, 485–499; (b) Ferretti, V.; Gilli, P.; Gavezzotti, A. X-ray diffraction and molecular

- simulation study of the crystalline and liquid state of succinic anhydride, *Chem. Eur. J.* 2002, **8**, 1710–1718.
- [7] Standard NPT-MD, GROMOS package, computational box of 400 benzene molecules ( $5 \times 4 \times 5$  unit cells), periodic boundary conditions, temperature, and isotropic pressure control, force field from a slight modification of the Williams potentials (ref. 44, Chapter 4), other working conditions as described in ref. [6].
- [8] Gavezzotti, A. A molecular dynamics test of the different stability of crystal polymorphs under thermal strain, *J. Am. Chem. Soc.* 2000, **122**, 10724–10725.
- [9] For a simple calculation based on the Lindemann criterion and comparison with experiment see for example Tabor, D. *Gases, Liquids and Solids*, 1969, Penguin Books, Baltimore, p. 207. The calculation assumes harmonic vibration of the particles, against Young's modulus. Melting temperatures are calculated with reasonable accuracy for metals and even for quartz, but not for organic molecules.
- [10] See for a description Frenken, J. W. M. *Surface melting*, Endeavour, New Series, 1990, **14**, 2; Dash, J. G. Surface melting, *Contemporary physics* 1989, **30**, 89. The occurrence of surface melting is the commonly accepted wisdom for metals and crystals of things like Ar and Ne. The presence of a liquid film on the surface of ice is given as an explanation of ice's slipperiness, but not without challenge.
- [11] A soft mode is a lattice mode whose frequency becomes imaginary at some value of the density (or external pressure). See e.g. Dove, M. T.; Rae, A. I. M. Structural phase transitions in malononitrile, *Faraday Disc.* 1980, **69**, 98–106. The whole discussion, entitled "Phase transitions in molecular solids", is extremely instructive reading for the theory, experiment, and simulation of second-order phase transitions, operatively defined as those transitions that occur without a major discontinuity in enthalpy and heat capacity: the onset of molecular rotation is an example, as opposed to first-order transitions like polymorphic transitions or melting.
- [12] McGann, M. R.; Lacks, D. J. Chain length effects on the thermodynamic properties of *n*-alkane crystals, *J. Phys. Chem. B* 1999, **103**, 2796–2802.
- [13] See for example Oxtoby, D. W. Nucleation of first-order phase transitions, *Acc. Chem. Res.* 1998, **31**, 91–97, and references therein. The classical nucleation theory (CNT) is challenged by extended theories, one of which was unfortunately called "density functional theory" because free energy is a functional of the average density profile of the nucleating site, generating some confusion, at least for theoretical chemists, with quantum chemical density functional theory.
- [14] See a critical analysis of the problem in Auer, S.; Frenkel, D. Quantitative prediction of crystal-nucleation rates for spherical colloids: a computational approach, *Annu. Rev. Phys. Chem.* 2004, **55**, 333–361. See also Turner, G. W.; Bartell, L. S. On the probability of nucleation at the surface of freezing drops, *J. Phys. Chem. A* 2005, **109**, 6877–6879, and references therein. These papers rely on a statistical analysis of simulated nucleation trajectories of clusters of SeF<sub>6</sub> molecules to estimate nucleation rates.

- [15] See, for example Wales, D. J.; Berry, R. S. Freezing, melting, spinodals and clusters, *J. Chem. Phys.* 1990, **92**, 4473–4482; the theory exposed there relies on the assumption of solid-like and liquid-like clusters coexisting in equilibrium at a given temperature, a rather curious assumption, at least for a molecular crystal chemist with a view on the complex kinetic interplay in molecular aggregations. In Hettema, H.; McFeaters, J. S. The direct Monte Carlo method applied to the homogeneous nucleation problem, *J. Chem. Phys.* 1996, **105**, 2816–2827, one reads that “the traditional definition of a ‘phase’ has limited meaning with respect to clusters”. If nucleation clusters are the key entities in solid–liquid equilibrium, we are led to the paradox of studying a phase equilibrium without a clear definition of the concept of phase.
- [16] Sainz-Diaz, C. I.; Martin-Islan, A. P.; Cartwright, J. H. E. Chiral symmetry breaking and polymorphism in 1,1'-binaphthyl melt crystallization, *J. Phys. Chem. B* 2005, **109**, 18758–18764.
- [17] For example: Yang, J.; Gould, H.; Klein, W.; Mountain, R. D. Molecular dynamics investigation of deeply quenched liquids, *J. Chem. Phys.* 1990, **93**, 711–723; van Duijneveldt, J. S.; Frenkel, D. Computer simulation study of free energy barriers to crystal nucleation, *J. Chem. Phys.* 1992, **96**, 4655–4668; Swope, W. C.; Andersen, H. C.  $10^6$ -particle molecular-dynamics study of homogeneous nucleation of crystals in a supercooled atomic liquid, *Phys. Rev.* 1990, **B41**, 7042–7054; Agrawal, R.; Kofke, D. A. Thermodynamic and structural properties of model systems at solid-fluid coexistence. II Melting and sublimation of the Lennard-Jones system, *Mol. Phys.* 1995, **85**, 43–59; Huitema, H. E. A.; Vlot, M. J.; van der Eerden, J. P. Simulations of crystal growth from Lennard-Jones melt: detailed measurements of the interface structure, *J. Chem. Phys.* 1999, **111**, 4714–4723; ten Wolde, P. R.; Ruiz-Montero, M.; Frenkel, D. Numerical calculation of the rate of crystal nucleation in a Lennard-Jones system at moderate undercooling, *J. Chem. Phys.* 1996, **104**, 9932–9947.
- [18] Brodka, A.; Zerda, T. W. Molecular dynamics simulation of liquid–solid phase transition of cyclohexane, *J. Chem. Phys.* 1992, **97**, 5669–5675; Esselink, K.; Hilbers, P. A. J.; van Beest, B. W. H. Molecular dynamics study of nucleation and melting of *n*-alkanes, *J. Chem. Phys.* 1994, **101**, 9033–9041. In this last paper, the crystallization of 156 model chains representing *n*-nonane is captured in a simulation, with an energy and density landscape that is exactly specular to the one shown in Fig. 13.1.
- [19] In a series of elegant experiments using electron diffraction on nuclei generated in a supersonic nozzle, together with molecular dynamics simulations, L. S. Bartell and coworkers have studied the nucleation rates of small globular molecules: see later discussion and ref. [65].
- [20] Polson, J. M.; Frenkel, D. Numerical prediction of the melting curve of *n*-octane, *J. Chem. Phys.* 1999, **111**, 1501–1510. The last sentence of this paper is: “with the rapid increase in computing power, calculations that are barely feasible now should be standard in a few years time”.

- [21] Matsumoto, M.; Saito, S.; Ohmine, I. Molecular dynamics simulation of the ice nucleation and growth process leading to water freezing, *Nature* 2002, **416**, 409–413. For typical *Nature* hype, see Sastry, S. Sculpting ice out of water, *Nature* 2002, **416**, 376–377.
- [22] Radhakrishnan, R.; Trout, B. L. Nucleation of hexagonal ice in liquid water, *J. Am. Chem. Soc.* 2003, **125**, 7743–7747.
- [23] Interestingly, the freezing process can be much more easily simulated in the presence of an external electric field: Svishchev, I. M.; Kusalik, P. G. Electrofreezing of liquid water: a microscopic perspective, *J. Am. Chem. Soc.* 1996, **118**, 649–654. The timescale for the transformation is calculated to be a few hundred picoseconds, or three orders of magnitude faster than the timescale found in the study of ref. [21].
- [24] Talanquer, V.; Oxtoby, D. W. Nucleation in molecular and dipolar fluids: interaction site model, *J. Chem. Phys.* 1995, **103**, 3686–3695. The phenomenological density functional theory is applied in conjunction with a simulation model including spherical objects interacting by Lennard-Jones and coulombic potentials.
- [25] See for example: (a) Sum, A. K.; Sandler, S. I.; Bukowski, R.; Szalewicz, K. Prediction of the phase behavior of acetonitrile and methanol with ab initio pair potentials, *J. Chem. Phys.* 2002, **116**, 7627–7636; (b) Lago, S.; Garzon, B.; Vega, C. Accurate simulations of the vapor-liquid equilibrium of important organic solvents and other diatomics, *J. Phys. Chem. B* 1997, **101**, 6763–6771. For empirical correlations between boiling points and molecular descriptors related to shape and hydrogen-bonding ability see Katritzky, A. R.; Mu, L.; Lobanov, V. S.; Karelson, M. Correlation of boiling points with molecular structure, *J. Phys. Chem.* 1996, **100**, 10400–10407.
- [26] (a) Alba-Simionesco, C.; Fan, J.; Angell, C. A. Thermodynamic aspects of the glass transition phenomenon. II. Molecular liquids with variable interactions, *J. Chem. Phys.* 1999, **110**, 5262–5272. (b) Alba, C.; Busse, L. E.; List, D. J.; Angell, C. A. Thermodynamic aspects of the vitrification of toluene and xylene isomers, and the fragility of liquid hydrocarbons, *J. Chem. Phys.* 1990, **92**, 617–624.
- [27] Morineau, D.; Alba-Simionesco, C. Hydrogen-bond-induced clustering in the fragile glass-forming liquid *m*-toluidine: experiments and simulations, *J. Chem. Phys.* 1998, **109**, 8494–8503.
- [28] Are some or all of these materials made of submicroscopic domains? The structural inhomogeneity is apparently parallel to dynamic inhomogeneity: “molecular rotation and translation may occur significantly faster in one part of the sample than in another part a few nanometers away”. Cicerone, M. T.; Ediger, M. D. Enhanced translation of probe molecules in supercooled o-terphenyl: signature of spatially heterogeneous dynamics? *J. Chem. Phys.* 1996, **104**, 7210–7218.
- [29] Chelli, R.; Cardini, G.; Procacci, P.; Righini, R.; Califano, S. Molecular dynamics of glass-forming liquids: structure and dynamics of liquid metatoluidine, *J. Chem. Phys.* 2002, **116**, 6205–6215.

- [30] Zannoni, C. Molecular design and computer simulations of novel mesophases, *J. Mater. Chem.* 2001, **11**, 2637–2646. Note that equation (3) in this reference should read:  $x = (\sigma_e^2 - \sigma_s^2)/(\sigma_e^2 + \sigma_s^2)$ . Edited by Pasini, P.; Zannoni, C. *Advances in the Computer Simulation of Liquid Crystals*, NATO Science Series C, Mathematical and physical sciences, Vol.545, 2000, Kluwer, Dordrecht.
- [31] Hulliger, J. Chemistry and crystal growth, *Angew. Chem. Int. Ed. Engl.* 1994, **33**, 143–162.
- [32] One such crystal addict was W. Koerner, who in the 1920s synthesized thousands of benzene derivatives and took a special pleasure in growing large crystals: see Demartin, F.; Filippini, G.; Gavezzotti, A.; Rizzato, S. X-ray diffraction and packing analysis on vintage crystals: Wilhelm Koerner's nitrobenzene derivatives from the School of Agricultural Sciences in Milano, *Acta Cryst.* 2004, **B60**, 609–620.
- [33] Ferrari, E. S.; Davey, R. J.; Cross, W. I.; Gillon, A. L.; Towler, C. S. Crystallization in polymorphic systems: the solution-mediated transformation of  $\beta$  to  $\alpha$  glycine, *Cryst. Growth Des.* 2003, **3**, 53–60 (optical microscopy, XRD, FT-IR); Cashell, C.; Corcoran, D.; Hodnett, B. K. Secondary nucleation of the  $\beta$ -polymorph of L-glutamic acid on the surface of  $\alpha$ -form crystals, *ChemComm* 2003, 374–375 (SEM imaging); Blagden, N.; Davey, R. J.; Lieberman, H. F.; Williams, L.; Payne, R.; Roberts, R.; Rowe, R.; Docherty, R. Crystal chemistry and solvent effects in polymorphic systems: sulfathiazole, *J. Chem. Soc. Faraday Trans.* 1998, **94**, 1035–1044 (morphology, XRD); Towler, C. S.; Davey, R. J.; Lancaster, R. W.; Price, C. J. Impact of molecular speciation on crystal nucleation in polymorphic systems, *J. Am. Chem. Soc.* 2004, **126**, 13347–53 (pH on zwitterionic aminoacid molecules).
- [34] Weissbuch, I.; Lahav, M.; Leiserowitz, L. Toward stereochemical control, monitoring and understanding crystal nucleation, *Cryst. Growth Des.* 2003, **3**, 125–150 and Weissbuch, I.; Leiserowitz, L.; Lahav, M. "Tailor-made" and charge-transfer auxiliaries for the control of the crystal polymorphism of glycine, *Adv. Mater.* 1994, **6**, 952–956 (additives; small angle XRD); Pino-Garcia, O.; Rasmuson, A. C. Influence of additives on nucleation of vanillin: experiments and introductory molecular simulations, *Cryst. Growth Des.* 2004, **4**, 1025–1037 (multicell crystallization with visual inspection).
- [35] Gracin, S.; Usi-Penttila, M.; Rasmuson, A. C. Influence of ultrasound on the nucleation of polymorphs of *p*-aminobenzoic acid, *Cryst. Growth Des.* 2005, **5**, 1787–1794, and Devarakonda, S.; Evans, J. M. B.; Myerson, A. S. Impact of ultrasonic energy on the crystallization of dextrose monohydrate, *Cryst. Growth Des.* 2003, **3**, 741–746 (increase in nucleation rate by ultrasound).
- [36] Lee, A. Y.; Lee, I. S.; Dette, S. S.; Boerner, J.; Myerson, A. S. Crystallization on confined engineered surfaces: a method to control crystal size and generate different polymorphs, *J. Am. Chem. Soc.* 2005, **127**, 14982–14983 (glycine on gold islands); Ha, J.-M.; Wolf, J. H.; Hillmyer, M. A.; Ward, M. D. Polymorph selectivity under nanoscopic confinement, *J. Am. Chem. Soc.* 2004, **126**, 3382–3383 (anthranilic acid on porous glass); Allen, K.; Davey, R. J.; Ferrari,

- E.; Towler, C.; Tiddy, G. J. The crystallization of glycine polymorphs from emulsions, microemulsions and lamellar phases, *Cryst. Growth Des.* 2002, **2**, 523–527 (optical microscopy and SEM).
- [37] Boerrigter, S. X. M.; van den Hoogenhof, C. J. M.; Meekes, H.; Bennema, P.; Vlieg, E.; van Hoof, P. J. C. M. In situ observation of epitaxial polymorphic nucleation of the model steroid methyl analogue 17-norethindrone, *J. Phys. Chem. B* 2002, **106**, 4725–4731; Bonafede, S. J.; Ward, M. D. Selective nucleation and growth of an organic polymorph by ledge-directed epitaxy on a molecular crystal substrate, *J. Am. Chem. Soc.* 1995, **117**, 7853–7861. (spectroscopy, microscopy).
- [38] Chen, S.; Xi, H.; Yu, L. Cross-nucleation between ROY polymorphs, *J. Am. Chem. Soc.* 2005, **127**, 17439–17444.
- [39] Aber, J. E.; Arnold, S.; Garetz, B. A.; Myerson, A. S. Strong DC electric field applied to supersaturated aqueous glycine solution induces nucleation of the  $\gamma$  polymorph, *Phys. Rev. Letters* 2005, **94**, 145503; Garetz, B. A.; Matic, J.; Myerson, A. S. Polarization switching of crystal structure in the nonphotochemical light-induced nucleation of supersaturated aqueous glycine solutions, *Phys. Rev. Letters* 2002, **89**, 175501.
- [40] Peters, R.; Georgalis, Y.; Saenger, W. Accessing lysozyme nucleation with a novel dynamic light scattering detector, *Acta Cryst.* 1998, **D54**, 873–877.
- [41] Wolk, J.; Strey, R. Homogeneous nucleation of H<sub>2</sub>O and D<sub>2</sub>O in comparison: the isotope effect, *J. Phys. Chem. B* 2001, **105**, 11683–11701.
- [42] Roelands, C. P. M.; Roestenberg, R. R. W.; ter Horst, J. H.; Kramer, H. J. M.; Jansens, P. J. *Cryst. Growth Des.* 2004, **4**, 921–928.
- [43] Mougin, P.; Wilkinson, D.; Roberts, K. J. In situ measurement of particle size during the crystallization of L-glutamic acid under two polymorphic forms: influence of crystal habit on ultrasonic attenuation measurements, *Cryst. Growth Des.* 2002, **2**, 227–234.
- [44] Groen, H.; Roberts, K. J. Nucleation, growth, and pseudo-polymorphic behavior of citric acid as monitored in situ by attenuated total reflection Fourier transform infrared spectroscopy, *J. Phys. Chem. B* 2001, **105**, 10723–10730. Coupled with turbidometric measurements, the results indicate a spontaneous liquid-phase separation prior to crystallization (“oiling-out”). See also Bonnett, P. E.; Carpenter, K. J.; Dawson, S.; Davey, R. J. Solution crystallisation via a submerged liquid–liquid phase boundary: oiling out, *ChemComm* 2003, 698–699.
- [45] Mohan, R.; Boateng, K. A.; Myerson, A. S. Estimation of crystal growth kinetics using differential scanning calorimetry, *J. Cryst. Growth* 2000, **212**, 489–499. See in this paper a brief review of some key references to analysis and control of crystallization processes in industrial applications.
- [46] Forland, G. M.; Liang, Y.; Kvalheim, O. M.; Hoiland, H.; Chazy, A. Associative behavior of benzyl alcohol in carbon tetrachloride solution, *J. Phys. Chem. B* 1997, **101**, 6960–6969.

- [47] Falcon, J. A.; Berglund, K. A. In situ monitoring of antisolvent addition crystallization with principal component analysis of Raman spectra, *Cryst. Growth Des.* 2004, **4**, 457–463.
- [48] Ono, T.; ter Horst, J. H.; Jansens, P. J. Quantitative measurement of the polymorphic transformation of L-glutamic acid using in-situ Raman spectroscopy, *Cryst. Growth Des.* 2004, **4**, 465–469.
- [49] Parveen, S.; Davey, R. J.; Dent, G.; Pritchard, R. G. Linking solution chemistry to crystal nucleation: the case of tetrolic acid, *ChemComm* 2005, **12**, 1531–1533.
- [50] Drenth, J.; Haas, C. Nucleation in protein crystallization, *Acta Cryst.* D1998, **54**, 867–872.
- [51] Spitaleri, A.; Hunter, C. A.; McCabe, J. F.; Packer, M. J.; Cockroft, S. L. A  $^1\text{H}$  NMR study of crystal nucleation in solution, *CrystEngComm* 2004, **6**, 489–493.
- [52] Chattopadhyay, S.; Erdemir, D.; Evans, J. M. B.; Ilavsky, J.; Amenitsch, H.; Segre, C. U.; Myerson, A. S. SAXS study of the nucleation of glycine crystals from a supersaturated solution, *Cryst. Growth Des.* 2005, **5**, 523–527.
- [53] Quayle, M. J.; Davey, R. J.; McDermott, A. J.; Tiddy, G. J. T.; Clarke, D. T.; Jones, G. R. In situ monitoring of rapid crystallization processes using synchrotron X-ray diffraction and a stopped-flow cell, *Phys. Chem. Chem. Phys.* 2002, **4**, 416–418.
- [54] See e.g. Watson, J. N.; Iton, L. E.; Keir, R. I.; Thomas, J. C.; Dowling, T. L.; White, J. W. TPA-silicalite crystallization from homogeneous solution: kinetics and mechanism of nucleation and growth, *J. Phys. Chem. B* 1997, **101**, 10094–10104.
- [55] Berkovitch-Yellin, Z. Toward an *ab initio* derivation of crystal morphology, *J. Am. Chem. Soc.* 1985, **107**, 8239–8253. The statement, coming from one of the founding members of the Weizmann school on crystal growth control, presumably refers to tailor-made impurities, but nevertheless sounds as a mourning bell for all theories of crystal formation based only on static energies and classical thermodynamics of pure systems.
- [56] See, for the basic ideas, the paper cited in ref. [55]; Clydesdale, G.; Docherty, R.; Roberts, K. J. HABIT—a program for predicting the morphology of molecular crystals, *Comp. Phys. Commun.* 1991, **64**, 311. For a discussion of the intrinsic shortcomings of these methods, see Roberts, K. J.; Docherty, R.; Bennema, P.; Jetten, L. A. M. The importance of considering growth-induced conformational change in predicting the morphology of benzophenone, *J. Phys. D Appl. Phys.* 1993, **26**, B7–B21.
- [57] See Grimbergen, R. F. P.; Meekes, H.; Bennema, P.; Strom, C. S.; Vogels, L. J. P. On the prediction of crystal morphology. I. The Hartman–Perdok theory revisited, *Acta Cryst.* 1998, **A54**, 491–500, and references therein. Periodic bond chains (PBC) define “flat” surfaces, as those surfaces with a compact structure that require energy for the formation of growth-promoting steps, while faces without PBCs are supposed to have a zero energy for step formation in some direction, and hence to be able to grow rough. These ideas have a certain amount of subjectivity, and such models, in their original formulation, neglect

some of the structural and energetic features typical of complex and flexible organic molecules.

Other variations on the theme of attachment energies include the use of quantum mechanical methods based on the crystal electron density for the calculation of attachment energies (Docherty, R.; Roberts, K. J.; Saunders, V.; Black, S.; Davey, R. J. Theoretical analysis of the polar morphology and absolute polarity of crystalline urea, *Faraday Discuss.* 1993, **95**, 11–25), or the modification of attachment energies by the inclusion of energy terms to represent the influence of impurities incorporated in the crystal lattice: Mougín, P.; Clydesdale, G.; Hammond, R. B.; Roberts, K. J. Molecular and solid state modeling of the crystal purity and morphology of caprolactam in the presence of synthesis impurities and the imino-tautomeric species caprolactim, *J. Phys. Chem. B* 2003, **107**, 13262–13272.

- [58] Boerrigter, S. X. M.; Hollander, F. F. A.; van der Streek, J.; Bennema, P.; Meekes, H. Explanation for the needle morphology of crystals applied to a triacylglycerol, *Cryst. Growth Des.* 2002, **2**, 51–54, with an approach to the calculation of the energies for step formation; Boerrigter, S. X. M.; Josten, G. P. H.; van der Streek, J.; Hollander, F. F. A.; Los, J.; Cuppen, H. M.; Bennema, P.; Meekes, H. MONTY: Monte Carlo crystal growth on any crystallographic orientation: application to fats, *J. Phys. Chem. A* 2004, **108**, 5894–5902; Deij, M. A.; Aret, E.; Boerrigter, S. X. M.; van Meervelt, L.; Deroover, G.; Meekes, H.; Vlieg, E. Experimental and computational growth morphology of two polymorphs of a yellow isoxazolone dye, *Langmuir* 2005, **21**, 3831–3837.
- [59] Cuppen, H. M.; Day, G. M.; Verwer, P.; Meekes, H. Sensitivity of morphology prediction to the force field: paracetamol as an example, *Cryst. Growth Des.* 2004, **4**, 1341–1349.
- [60] ter Horst, J. H.; Geertman, R. M.; van Rosmalen, G. M. The effect of solvent on crystal morphology, *J. Cryst. Growth* 2001, **230**, 277–284.
- [61] For an introduction see Palmore, G. T. R.; Luo, T. J.; Martin, T. L.; McBride-Wieser, M. T.; Voong, N. T.; Land, T. A.; De Yoreo, J. J. Using the atomic force microscope to study the assembly of molecular solids, *American Crystallographic Association Transactions* 1998, **33**, 45–57. For applications see Malkin, A. J.; Kuznetsov, Y. G.; Glantz, W.; McPherson, A. Atomic force microscopy studies of surface morphology and growth kinetics in thaumatin crystallization, *J. Phys. Chem.* 1996, **100**, 11736–11743; Wen, H.; Li, T.; Morris, K. R.; Park, K. Dissolution study on aspirin and  $\alpha$ -glycine crystals, *J. Phys. Chem. B* 2004, **108**, 11219–11227; Luo, T.-J.; MacDonald, J. C.; Palmore, G. T. R. Fabrication of complex crystals using kinetic control, chemical additives, and epitaxial growth, *Chem. Mater.* 2004, **16**, 4916–4927; Abendan, R. S.; Swift, J. A. Dissolution on cholesterol monohydrate single-crystal surfaces monitored by in situ atomic force microscopy, *Cryst. Growth Des.* 2005, **5**, 2146–2153.
- [62] See, for a clear review of these problems, Kotrla, M. Numerical theories in the simulation of crystal growth, *Comp. Phys. Commun.* 1996, **97**, 82–100.

- [63] Boek, E. S.; Briels, W. J.; Feil, D. Interfaces between a saturated aqueous urea solution and crystalline urea: a molecular dynamics study, *J. Phys. Chem.* 1994, **98**, 1674–1681; Hussain, M.; Anwar, J. The riddle of resorcinol crystal growth revisited: molecular dynamics simulation of  $\alpha$ -resorcinol crystal-water interface, *J. Am. Chem. Soc.* 1999, **121**, 8583–8591.
- [64] Datta, S.; Grant, D. J. W. Computing the relative nucleation rate of phenylbutazone and sulfamerazine in various solvents, *Cryst. Growth Des.* 2005, **5**, 1351–1357. This study uses a few solute molecules and 20–100 solvent molecules.
- [65] Chushak, Y.; Bartell, L. S. Crystal nucleation and growth in large clusters of  $\text{SeF}_6$  from molecular dynamics simulations, *J. Phys. Chem. A* 2000, **104**, 9328–9336. The study required nanosecond simulation for 10–12 clusters of up to 2,085 molecules at many temperatures, using a 7-site atom–atom potential and rigid-body molecular dynamics, in which the equations of motion are solved in three positional and three orientational coordinates for each molecule. Nucleation and crystallization were clearly observed.
- [66] Ding, F.; Bolton, K.; Rosen, A. Nucleation and growth of single-walled carbon nanotubes: a molecular dynamics study, *J. Phys. Chem. B* 2004, **108**, 17369–17377.
- [67] Huitema, H. E. A.; van Hengstum, B.; van der Eerden, J. P. Simulation of crystal growth from Lennard-Jones solutions, *J. Chem. Phys.* 1999, **111**, 10248–10260.
- [68] For applications to vapor–liquid nucleation see McKenzie, M. E.; Chen, B. Unravelling the peculiar nucleation mechanism for non-ideal binary mixtures with atomistic simulations, *J. Phys. Chem. B* 2006, **110**, 3511–3516; Chen, B.; Siepmann, J. I.; Klein, M. L. Simulating the nucleation of water/ethanol and water/nonane mixtures, mutual enhancement and two-pathway mechanism, *J. Am. Chem. Soc.* 2003, **125**, 3113–3118. The latter paper has a reference and discussion to experimental measurements using a supersonic nozzle expansion technique.